Consequences of Conical Intersections in the H + O_2 → OH + O Reaction?

Ruian Fei, Xiaonan S. Zheng,[1] and Gregory E. Hall*

Chemistry Department, Brookhaven National Laboratory, Upton, New York 11973-5000

Received: October 25, 1996; In Final Form: January 29, 1997[⊗]

Doppler-resolved laser-induced fluorescence spectroscopy of the OH reaction products of the photoinitiated reaction H + O_2 → OH + O has been applied at collision energies near 1.8 eV, where an anomalous peak in the total reaction cross section has been reported by Kessler and Kleinermanns (*J. Chem. Phys.* **1992**, *97*, 374). Although the product state distributions show no remarkable variation as the collision energy varies through this region, analysis of the Doppler line shapes suggests a sideways scattering component to the differential cross sections near 1.8 eV that is not present at higher collision energies. We propose that the qualitative change in the differential cross sections as well as the local peak in the integral cross section can be a consequence of the dynamics in the vicinity of the C_{2v} conical intersection.

I. Introduction

As an endothermic and chain-branching reaction, accounting for a major fraction of the initial activation of O_2 in most combustion systems, the reaction of H atoms with O_2 has attracted the attention of a large number of experimental and theoretical chemists and combustion scientists. A great deal is consequently known about this reaction. Thermal rate constants over a wide range of temperatures and pressures are required at very high precision in order to model ignition and flame propagation correctly. Recent high-temperature shock tube/flash absorption measurements have been combined with a critical review of experimental work on thermal rate constants for this reaction by Du and Hessler.[2] The reaction has also been extensively studied using photochemical H atoms and state-resolved product detection by laser-induced fluorescence (LIF). Product state distributions for both OH ($^2\Pi_\Omega$)[3−8] and O (^3P_J)[9,10] have been measured at numerous collision energies in excess of the 0.7 eV threshold for reaction. Doppler spectroscopy applied to the single-collision OH reaction products has been analyzed in this laboratory[11] to infer a differential cross section (DCS) for reactions at 2.3 eV that peaks in the forward direction (OH parallel to H) with a weaker backward component and an interesting variation in the rotational polarization of the OH that depends on the Λ-doublet state.

One remaining puzzle is the reported sharp maximum in the total reaction cross section at collision energies near 1.8 eV, as derived from measurements of OH LIF intensity in a scan of the HI photodissociation wavelength by Kessler and Kleinermanns.[12] After corrections were made for laser intensities, HI absorption cross sections, I/I* branching ratios, the fractional yield of OH in the detected level, and the H atom velocity, the OH signals were transformed to the collision energy-dependent cross sections shown in the top panel of Figure 1, adapted from Kessler and Kleinermanns.[12] The reaction cross section is reported to rise by a factor of 4 between 1.6 and 1.8 eV collision energy and to fall again by a factor of 3 at collision energies above 2.2 eV. This remarkable result is not reproduced by any quasiclassical trajectory calculations,[6,12−15] quantum calculations[17−19] until recently, and has puzzled most of us who have cared about the H + O_2 reaction. It has inspired successful experimental replication,[20] and several unsuccessful theoretical attempts to explain the result[16,17,19,21] within the framework of a single, adiabatic potential surface. A recent classical approach by Varandas[22] for extrapolating the $J = 0$ quantum mechanical reactive probability to include higher total J has succeeded in generating a peak in the energy-dependent total cross section. In this work, classical trajectories are used to compute the maximum reactive impact parameter, b_{max}, at each collision energy, which is then used in an approximate scaling of the quantum $J = 0$ excitation functions to include total J up to about

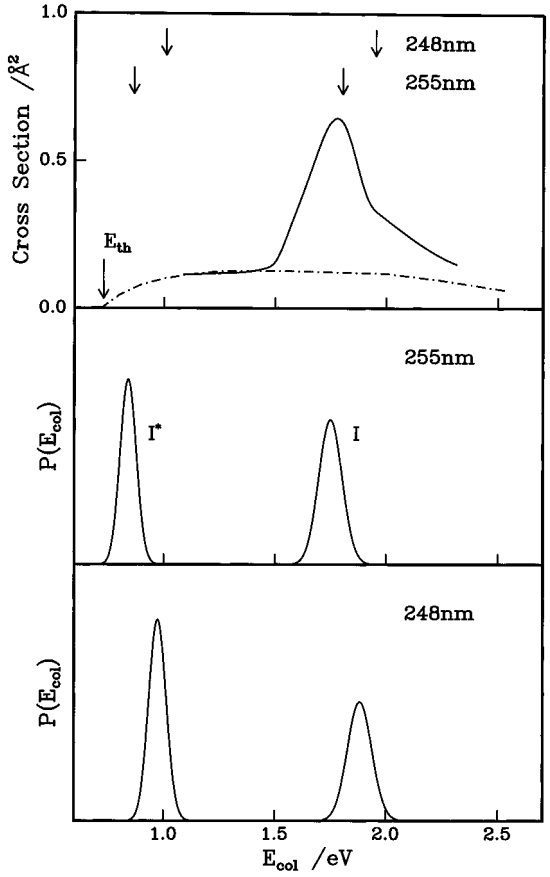

Figure 1. Energy dependent integral reactive cross section for H + O_2 → OH + O. Top panel: solid line adapted from experimental results of Kessler and Kleinermanns;[12] E_{th} depicts the energy threshold for reaction; dot-dashed line schematically depicts typical calculated integral cross sections from classical trajectory methods.[13,14,16] Arrows indicate average collision energies accessed for HI photodissociation at 248 and 255 nm. Lower panels: distribution of collision energies in the c.m. for 255 and 248 nm photolysis of thermal HI/O_2 mixtures.

[⊗] Abstract published in *Advance ACS Abstracts*, March 15, 1997.

S1089-5639(96)03334-8 CCC: $14.00

60. An energy dependence of b_{max} included in this most recent work[21] can generate a local maximum in the calculated integral cross section, which had not been obtained in an earlier, simpler version of this approximation.[21]

We have applied methods of Doppler spectroscopy to the OH products of this reaction at collision energies near the cross section anomaly, in an attempt to understand its source. Indeed, there appears to be a qualitative change in the differential cross sections in the vicinity of 1.8 eV, and we suggest that both the integral and the differential cross sections may be related to dynamical consequences of the C_{2v} conical intersection calculated to lie near this energy.[23]

II. Experimental Section

The experimental approach is similar to that reported earlier.[11] Sample gas mixtures of 1:1 HI:O_2 were slowly flowed at a total pressures of 50 mTorr at room temperature through a sample chamber and subjected to a photolysis-react-probe sequence with a 50 ns delay between orthogonal photolysis and probe laser beams. Fluorescence from newly formed OH reaction products was detected with no polarization selection at right angles to the laser beams for different combinations of linear polarization directions for the two laser beams. To produce H atoms with a center-of-mass (c.m.) collision energy peaked near 1.8 eV, we used a frequency-doubled dye laser (Lambda Physik 3002), pumped by a 308 nm excimer laser (Questek 2340), to photodissociate HI at 255 nm. Comparisons were also made with the photolysis laser tuned to 257 and 248 nm and an excimer laser running at 248 nm. The OH reaction products were detected by LIF on the 0−0 band of the $A-X$ transition, using a single-longitudinal mode pulsed dye laser (Lumonics HD-300-SLM) pumped by a frequency-doubled Nd:YAG laser. Second-harmonic light from DCM near 310 nm had a measured line width (Burleigh RC300) less than 0.02 cm^{-1} fwhm. Since our previous report we are now using a photoelastic modulator (Hinds PEM-II) to measure interleaved Doppler scans in two polarizations, acquiring 10 Hz spectra with alternate photolysis or probe laser polarizations changing from horizontal to vertical linear polarization. The LIF signal was collected through f/2 optics and filtered with a 10 nm bandwidth interference filter centered at 313 nm, to collect the 0−0 band OH fluorescence and reject a background fluorescence due to the photolysis laser excitation of an I_2 contaminant. The HI (Matheson) was distilled between glass traps and introduced to the sample chamber through Teflon tubing from a dry ice-cooled trap. The I_2 background was significantly reduced by this procedure, although even with the interference filter, 248 nm photolysis energies in excess of a few millijoules could not be used.

Multiple scans were averaged in each geometry for selected rotational lines, using a simultaneously acquired I_2 LIF calibration spectrum from the probe laser fundamental to register the coadded OH LIF scans. The spectra shown in Figures 2 and 3 represent 5000−10000 laser shots of signal averaging per 0.02 cm^{-1} line width of the probe laser. Error bars reflect 1σ errors in the mean at each Doppler shift.

III. Results and Analysis

Doppler-broadened LIF spectra of the products of photoinitiated reactions, measured in multiple geometries on different rotational branches, can reveal a highly detailed account of the reactive event. In addition to our previous work on this reaction at higher collision energies,[11] the method has been developed primarily in the laboratories of Simons and Zare, each of whom has recently produced a highly readable review of this extension

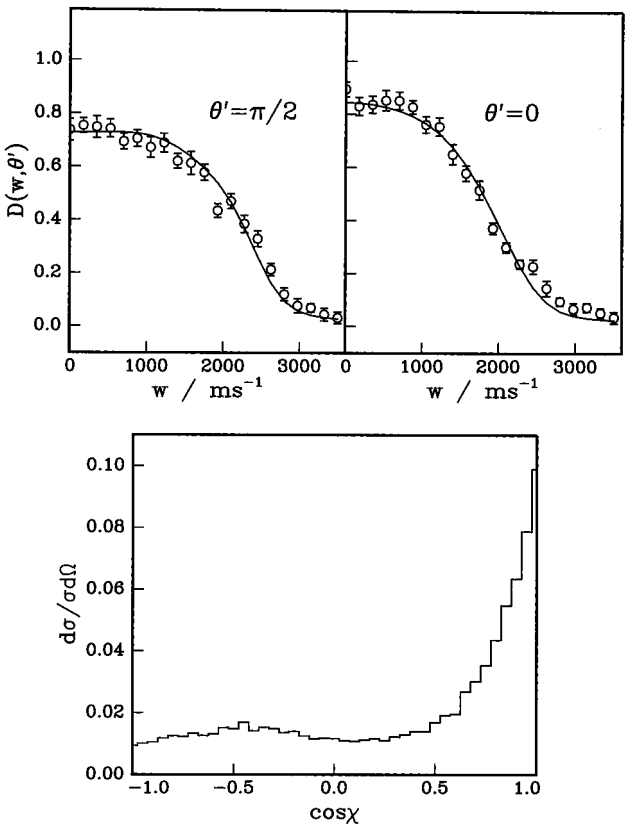

Figure 2. Doppler profiles and fits to nascent OH reaction products following 248 nm photolysis of HI. Upper panels: $Q_1$14 with Doppler shifts expressed as velocity, for two experimental geometries. Solid line is maximum entropy fit, derived from the DCS shown in the lower panel.

of vector correlation measurements into the collisional domain.[24−26]

On the basis of our earlier measurements and analysis of the 2.3 eV H + O_2 collisions, the difference in the rotational polarization properties of the two Λ doublets makes the composite line shape/Fourier transform method of Aoiz *et al.*[27] unsuitable for the extraction of differential cross sections or vector correlations in these experiments. The strongly populated rotational levels of OH are at high enough rotational levels, N, that the satellite branches are too weak to measure, spoiling another possible approach to measuring Q- and R-type transitions from *each* Λ doublet, as has been done for the $v = 0$, $N = 5$ OH product in the O (^{1}D) + CH_4 reaction, recently studied in the laboratory of Simons.[28] We therefore continue to use the analysis method described earlier,[11] where differential cross sections are derived by direct inversion of Doppler line shapes acquired in several geometries, subject to a trial-and-error variation in the rotational polarization properties of each Λ doublet. The signal-to-noise ratio for the present data, acquired with a reduced photolysis laser energy and a H atom precursor with smaller absorption compared to our previous study, is unfortunately insufficient for a complete and independent analysis. A direct comparison between measurements made at nearby dissociation wavelengths can still be made, however, focusing on the differential cross sections, assuming that the rotational polarization properties are independent of the collision energy over the narrow range of interest. While this assumption has not been fully tested, subsequent alignment measurements have been made that are consistent with this assumption, although the errors are large enough to leave open the possibility of other interpretations. The differential cross sections, in any case, generally have a stronger influence on the observed

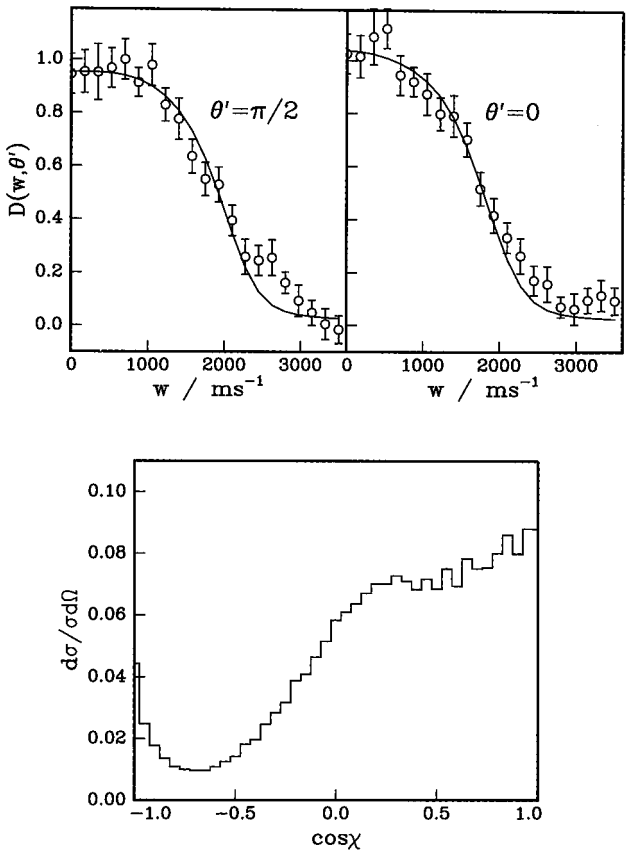

Figure 3. Doppler profiles and fits to nascent OH reaction products following 255 nm photolysis of HI.

Doppler profiles than the rotational polarization properties of the reaction products.[11,24,26]

The lower panels of Figure 1 illustrate the distribution of c.m. collision energies for 255 and 248 nm photolysis of HI, including the room temperature velocity distributions of HI and O_2. The faster H atoms have average collision energies of 1.8 and 1.9 eV at these photolysis energies, which should sample near the peak, and beyond the peak in the total cross section. The slower H atoms, produced in coincidence with excited iodine atoms, produce H + O_2 collisions just above the 0.7 eV threshold for the reaction and contribute only to the lower rotational levels of OH.

An analysis identical to that described in ref 11 was applied to $Q_1$14 and $P_1$14 lines, each measured in two geometries at 248 and at 255 nm. The Doppler profiles did not change significantly with changes in the probe laser polarization; the majority of the measurements were made with the probe laser polarization set along the direction toward the photomultiplier tube. The photolysis laser was alternately polarized perpendicular and parallel to the probe propagation direction. A simultaneous fit to both geometries for both Q and P lines was performed with the maximum entropy procedure of ref 11 at each collision energy. Figures 2 and 3 show the $Q_1$14 Doppler profiles with the probe parallel ($\theta' = 0$) and perpendicular ($\theta' = \pi/2$) to the photolysis polarization, the optimum fits, and the associated differential cross sections. The half-Doppler profiles have been plotted on a velocity scale, with *w* the component of the OH laboratory velocity along the Doppler probe propagation direction. The differential cross sections are plotted with respect to the cosine of the c.m. scattering angle, χ, defined such that $\chi = 0$ ($\cos\chi = 1$) is forward scattering of the OH in the same direction as the H reactant. The collision frame rotational polarization has been assumed to be the same as was derived from the earlier analysis of the 2.3 eV collisions.[11] That is, the $\Pi(A'')$ Λ doublets, probed by Q-branch lines, are unpolarized, and the $\Pi(A')$ Λ doublets, probed by P- and R-branch lines, are strongly polarized, with their rotation axis sharply perpendicular to their asymptotic c.m. velocity. Our experience in fitting the higher quality Doppler profiles at 2.3 eV was that the main effect of different assumed forms or magnitudes of the rotational polarization is to modify the quality of the fits, but not to make qualitative changes in the derived differential cross sections. At 1.8 eV, the DCS appears to have a broad component of sideways scattering that is missing at 1.9 eV. This qualitative difference between the DCS at 1.8 and 1.9 eV was consistently produced with fits to either the separate or combined Q- and P-branch data. The presence of the sideways scattering is evident in the raw data as a smaller difference between the Doppler profiles in the two geometries, due to the more isotropic reactive scattering.

The combination of lower photolysis energies and smaller absorption cross sections for HI compared to H_2S makes these Doppler profiles noisier than our earlier data, despite extensive signal averaging. Given the subtlety of the analysis and the noise in the data, one is obviously led to question the confidence in the result. Error bounds are notoriously difficult to assign to the results of a maximum entropy optimization. We instead apply a χ^2 test[29] to the null hypothesis that the 1.8 eV data could be a random sample from a distribution of possible noisy Doppler spectra with an underlying DCS identical to the one derived from better data at 1.9 eV collision energy, that is, lacking the sideways component. A reduced χ^2 for the null hypothesis is 1.6, with 40 degrees of freedom, unlikely at the 99% confidence level. The maximum entropy solution for the 1.8 eV DCS leads to a reduced χ^2 of 1.18. A deviation this large would occur by chance with a probability of 0.2 if the optimum DCS were exact. We conclude that the sideways component in the DCS at 1.8 eV is implied by the data, although some of the residual error is likely to be systematic.

To test for possible systematic differences between the 248 nm (excimer laser) and the 255 nm (doubled dye laser) experiments, we repeated the 248 nm experiments with the frequency-doubled dye laser tuned to 248 nm, under experimental conditions identical to the 255 nm measurements. Apart from an increased noise level at the weaker photolysis energy, the Doppler profiles were similar, and the maximum entropy fits to the DCS still lacked the sideways component, as previously observed with the excimer laser experiments.

Measurements of the relative intensities of the Doppler-integrated LIF lines in different geometries provided further checks on both the assumed pattern of OH rotational polarization and the DCS derived from the Doppler analysis. The intensity ratio depends on $\langle P_2(\hat{z}\cdot\hat{j})\rangle$, the ensemble average over all OH final velocities of the second Legendre moment of the cosine of the angle between the OH rotation vector and the body-fixed reference direction, *z*, parallel to the initial H atom velocity. Our earlier intensity measurements[11] at 2.3 eV collision energy had led to velocity-averaged values of the $\beta_0^2(02)$ bipolar moment (equal to $\langle P_2(\hat{z}\cdot\hat{j})\rangle$) of -0.56 ± 0.15 for the strongly polarized P- and R-branch lines, probing the Π (A′) Λ doublets, and -0.09 ± 0.12 for the nearly depolarized Q-branch lines, probing the Π (A″) Λ doublets. If our assumption of an energy-independent collision-frame rotational polarization for the Π (A′) Λ doublets is correct, characterized only by a cylindrically symmetric correlation between the OH rotation and the *final* velocity of the OH, we should see a reduced magnitude of the *laboratory frame* alignment if the DCS includes a significant sideways scattering component. The Π (A″) Λ doublets should continue to have no significant rotational polarization in any

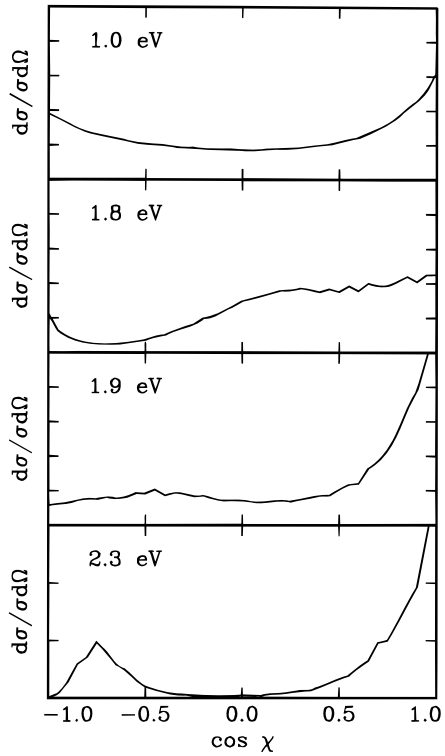

Figure 4. Selection of collision energy-dependent differential cross sections derived from Doppler spectroscopy. The detected states (all OH $v = 0$) used were $N = 4$ at 1.0 eV, $N = 14$ at 1.8 eV and 1.9 eV, and $N = 17$ at 2.3 eV, in each case near the maximum of the OH state distribution.

frame, and the intensity ratio measurements should be insensitive to any changes in the DCS. Repeating the intensity measurements for 1.8 eV collisions led to corresponding bipolar moments of -0.32 ± 0.40 and -0.02 ± 0.07 for A′ and A″ Λ components, respectively. The A″ Λ doublets remain unpolarized, and we can rule out changes in the rotational polarization as being responsible for the change in their Doppler profiles. This strengthens the case for the sideways component to the DCS. As strong a case cannot be made from our measurements of the A′ Λ doublets, where an observed reduction in the magnitude of the velocity-averaged $\beta_0^2(02)$ bipolar moment would have supported our interpretation of energy-independent collision-frame polarization and an energy-dependent DCS. The experimental results are not inconsistent with this prediction, yet neither are they good enough to confirm it.

We also compared the relative intensities of Q_1 14 lines at these two photolysis wavelengths, attempting to verify the energy-dependent integral cross sections first reported by Kessler and Kleinermanns.[12] In tuning from 248 to 255 nm, the HI absorption cross section decreases[30] by 30%, the quantum yield of I ($^3P_{3/2}$) increases[31] by 5%, and the relative collision velocity decreases by 3%. After small linear corrections for photolysis laser energies, the integrated OH signal for $v = 0$, $N = 14$ was larger by 20% at 255 nm. The OH state distributions are similar, from which we derive about a 50% increase in the total reactive cross section from 1.9 to 1.8 eV, in qualitative agreement with previous measurements depicted in Figure 1.

A survey of collision energy-dependent differential cross sections, derived from Doppler analysis of the H + O_2 reaction, is shown in Figure 4. The 1.0 eV collision energy DCS was derived from the slow H channel of the 248 nm HI experiment, probing OH $v = 0$, $N = 4$. The overlapping contribution of 1.9 eV collisions to the $N = 4$ Doppler profiles is much broader and accounts for only about 10% of the total signal, allowing a clean separation of the two formation paths. At 1.0 eV, the DCS is more symmetric in the forward/backward directions, as would be expected for a rotationally persistent HO_2 complex intermediate. Neither Λ doublet component was found to be strongly polarized at this collision energy, and good fits were obtained for both Q and P, branches assuming no rotational polarization. The 1.8 and 1.9 eV differential cross sections described above are shown, along with the 2.3 eV DCS from our earlier work.[11]

IV. Discussion

The quality of our present data and the complexity of the analysis do not, unfortunately, permit us to consider these results as conclusive. The pattern of energy-dependent changes in the DCS is, however, highly suggestive of an intuitively satisfactory interpretation, which we hope will encourage new theoretical or experimental lines of thought. A sensible argument can be made for the appearance and disappearance of a sideways component to the DCS at and above 1.8 eV, based on a transition from adiabatic to diabatic collisions at and above the energy of the C_{2v} conical intersection, an elaboration of a conjecture originally made by Varandas[16] in 1993.

The lowest energy $^2A''$ state of HO_2 correlates adiabatically with both H (^2S) + O_2 ($^3\Sigma^-_g$) and to OH ($^2\Pi$) + O (^3P) along a reaction path with no barriers other than the 0.7 eV reaction endothermicity. Much of the published theoretical work on this reaction has therefore been devoted to characterizing this surface and the dynamics it can mediate. Barriers do exist, in both the linear and the T-shaped approach channels, the result of intersecting $^2\Sigma^-$ and $^2\Pi$ surfaces in $C_{\infty h}$ symmetry and $^2A_2$ and $^2B_1$ surfaces in C_{2v} symmetry. Recent theoretical work on representing the multiple surfaces of HO_2,[32,33] the vibrational dynamics,[34,35] and the low-energy inelastic scattering[36] of H on O_2, have explored some consequences of the conical intersections, particularly the C_{2v} intersection. Orbits of the H atom around the intersection are energetically accessible even in the bound HO_2 molecule, leading to a Berry phase contribution to the vibrational dynamics[35] and recombination resonances.[36] As the translational energy becomes comparable to the energy of the intersection, calculated to be about 1.7 eV above the reactant zero-point energy,[23] one might look for dynamic consequences in the reaction dynamics as well.

A rotationally sudden limit provides a useful qualitative framework for visualizing the differential cross section at high collision energies, particularly for the L + HH mass combination. The thermal rotational velocity of O_2 is slow compared to the approach velocity of 1.8 eV hydrogen atoms. For a direct reaction, the asymptotic O + OH relative velocity will be close to the O−O bond direction at the time of reaction. In this limit, the DCS can be considered a measure of the dependence of the reaction probability on the polar approach angle. The absence of sideways scattering in the high-energy collision can be taken as an indication that the side-on H atom approach is nonreactive. The relatively small cross section at high energy has been attributed to a restricted range of reactive approach directions in early quasi-classical trajectory work by Kleinermanns and Schinke.[14] Similar conclusions have been drawn from trajectories on an improved DBME IV surface by Varandas.[16] In the same spirit, the increase in the integral cross section near 1.8 eV is consistent with the onset of a sideways component to the reactivity, where a larger fraction of possible approach geometries are reactive. We should emphasize that at 1.8 eV, the collisions are already more than 1 eV above the reaction threshold, and the resonances that dominate the near-threshold reaction have given way to what appears to be a more direct

mechanism, based on the changing state distributions.[5,6] At lower energies, where resonances dominate the reaction dynamics, departures from the rotationally sudden limit are expected, and the differential cross sections should not be expected to simply reflect the distribution of reactive approach directions. Indeed, the average DCS for a range of collision energies near 1.0 eV appears to show the forward−backward symmetry expected from long-lived complexes and has nothing to do with the polar approach angles.

We propose, following the conjecture of Varandas,[16] that at collision energies below the C_{2v} intersection, the adiabatic barrier prevents reaction for sideways approach directions. The reactive collisions at 1 eV are primarily complex forming, and the experimental DCS includes scattering at all angles, with no strong rotational polarization effects. As the collision energy approaches the conical intersection, near-sideways approach surmounts the adiabatic barrier to the HO_2 complex, passing through the crossing region at low velocity and following the adiabatic path to the complex and on to products. The opening of the range of reactive approach coordinates can result in an abrupt increase in the sideways component of the DCS, as well as an increase in the integral cross section. At energies above the intersection, even though the energy is sufficient to surmount the adiabatic barrier to reaction for near-sideways approach, the velocity through the crossing region can be high enough to force the collision along the repulsive diabatic curve resembling the $^2B_1$ electronic configuration for approach angles close to 90°, thus closing the window on the sideways approach reactivity. Calculations including the relevant surfaces and their nonadiabatic couplings to test this proposal appear to be possible, although challenging.

We note that our high-energy DCS shows substantially less backward scattering of OH than the single-surface classical trajectory calculations, which, if the present multisurface conjecture is correct, should not give a quantitatively correct description of the reaction. Some additional support for this result comes from the O atom Doppler profiles reported by Matsumi *et al*.[9] As recently noted by Seeger *et al*.,[20] the c.m. kinetic energy release derived from the O atom Doppler profiles is less than that calculated directly from the measured OH state distributions at 1.9 and 2.5 eV collision energy. The analysis of Matsumi *et al*. relied on trajectory calculations[14] to justify the use of an isotropic model for the extraction of an average c.m. kinetic energy release from the laboratory velocity measurements. If the OH is indeed preferentially forward scattered relative to the H velocity, then, of course, the O must be backward scattered, which will make the measured O Doppler profiles narrower than if they had been isotropically scattered at the same c.m. kinetic energy. The effect is large enough to reconcile their observations with the measured OH state distributions.

V. Conclusion

The H + O_2 → OH + O reaction has been examined at collision energies near 1.8 eV using Doppler spectroscopy. Energy-dependent trends in the differential cross sections derived from the Doppler spectra shows signs of sideways scattering that are lacking at higher collision energies. The measurements support a conjecture of Varandas[16] that the abrupt decline in the total reactive cross section above 1.8 eV can be due to repulsive interactions along an A″ diabatic entrance channel resembling the lowest $^2B_1$ state of HO_2 in geometries close to C_{2v} symmetry. Theoretical progress is rapid in this system, and with new representations of the multiple surfaces and increasingly sophisticated quantum scattering methods becoming accessible, we may hope for a deeper understanding of this important, and surprisingly complex, elementary reaction.

Acknowledgment. It is a pleasure to acknowledge useful discussions with Dr. R. T. Pack and Prof. A. J. C. Varandas. This work was performed at Brookhaven National Laboratory under Contract DE-AC02-76CH00016 with the U.S. Department of Energy and supported by its Division of Chemical Sciences.

References and Notes

(1) Present address: Department of Earth and Atmospheric Sciences, Georgia Institute of Technology, Atlanta, GA 30332-0340.
(2) Du, H.; Hessler, J. P. *J. Chem. Phys.* **1992**, *96*, 1077.
(3) Kleinermanns, K.; Wolfrum, J. *J. Chem. Phys.* **1984**, *80*, 1446.
(4) Kleinermanns, K.; Linnebach, E. *J. Chem. Phys.* **1985**, *82*, 5012.
(5) Bronikowski, M. J.; Zhang, R.; Rakestraw, D. J.; Zare, R. N. *Chem. Phys. Lett.* **1989**, *156*, 7.
(6) Kleinermanns, K.; Linnebach, E.; Pohl, M. *J Chem. Phys.* **1989**, *91*, 2181.
(7) Hall, G. E.; Sears, T. J. *Chem. Phys. Lett.* **1989**,*158*, 184.
(8) Jacobs, A.; Volpp, H. R.; Wolfrum, J. *Chem. Phys. Lett.* **1991**, *177*, 200.
(9) Matsumi, Y.; Shafer, N.; Tonokura, K.; Kawasaki, M.; Kim, H. L. *J. Chem. Phys.* **1991**, *95*, 4972.
(10) Rubahn, H.; van der Zande, W. J.; Zhang, R.; Bronikowski, M. J.; Zare, R. N. *Chem. Phys. Lett.* **1991**, *186*, 154.
(11) Kim, H. L.; Wickramaaratchi, M. A.; Zheng, X.; Hall, G. E. *J. Chem. Phys*. **1994**, *101*, 2033.
(12) Kessler, K.; Kleinermanns, K. *J. Chem. Phys.* **1992**, *97*, 374.
(13) Miller, J. A. *J. Chem. Phys.* **1981**, *74*, 5120.
(14) Kleinermanns, K.; Schinke, R. *J. Chem. Phys.* **1984**, *80*, 1440.
(15) Varandas, A. J. C.; Brandão J.; Pastrana, M. R. *J. Chem. Phys.* **1992**, *96*, 5137.
(16) Varandas, A. J. C. *J. Chem. Phys.* **1993**, *99*, 1076.
(17) Pack, R. T.; Butcher, E. A.; Parker, G. A., *J. Chem. Phys.* **1993**, *99*, 9310; **1995**, *102*, 5998.
(18) Leforestier, C.; Miller, W. H. *J. Chem. Phys.* **1994**, *100*, 733.
(19) Zhang, D. H.; Zhang, J. Z. H. *J. Chem. Phys.* **1994**, *101*, 2671.
(20) Seeger, S.; Sick, V.; Volpp, H. R.; Wolfrum, J. *Isr. J. Chem.* **1994**, *34*, 5.
(21) Varandas, A. J. C. *Chem. Phys. Lett* **1995**, *235*, 111.
(22) Varandas, A. J. C. *Mol. Phys.* **1995**, *85*, 1159.
(23) Walch, S. P.; Rohlfing, C. M. *J. Chem. Phys.* **1989**, *91*, 2373.
(24) Brouard, M.; Simons, J. P. In *Chemical Dynamics and Kinetics of Small Radicals*; Wagner, A., Liu, A., Eds.; World Scientific Publications: Singapore, 1995.
(25) Orr-Ewing, A. J.; Zare, R. N. In *Chemical Dynamics and Kinetics of Small Radicals*; Wagner, A., Liu, K., Eds.; World Scientific Publications: Singapore, 1995.
(26) Orr-Ewing, A. J.; Zare, R. N. *Annu. Rev. Phys. Chem.* **1994,** *45*, 315.
(27) Aoiz, F. J.; Brouard, M.; Enriquez, P. A.; Simons, J. P. *J. Chem. Soc., Faraday Trans.* **1993**, *89*, 1435.
(28) Brouard, M.; Lambert, H. M.; Short, J.; Simons, J. P. *J. Phys. Chem.* **1995**, *99*, 13571.
(29) Bevington, P. R. *Data Reduction and Error Analysis for the Physical Sciences*; McGraw-Hill: New York, 1969.
(30) Huebert, B. J.; Martin, R. M. *J. Phys. Chem.*, **1968**, *72*, 3046.
(31) van Veen, G. N. A.; Mohamed, K. A.; Baller, T.; de Vries, A. E. *Chem. Phys.* **1983** *80*, 113.
(32) Kendrick, B; Pack, R. T *J. Chem. Phys.* **1995**, *102*, 1994.
(33) Varandas, A. J. C.; Voronin, A. I. *J. Phys. Chem.* **1995**, *99*, 15846.
(34) Barclay, V. J.; Dateo, C. E.; Hamilton, I. P. *J. Chem. Phys.* **1994**, *101*, 6766.
(35) Barclay, V. J.; Dateo, C. E.; Hamilton, I. P.; Kendrick, B.; Pack, R. T.; Schwenke, D. W. *J. Chem. Phys.* **1995**, *103*, 3864.
(36) Kendrick, B., Pack, R. T. *J. Chem. Phys.* **1996**, *104*, 7475; 7502.